Preparation and characterisation of solvent-stabilised nanoparticulate platinum and palladium and their catalytic behaviour towards the enantioselective hydrogenation of ethyl pyruvate

Paul J. Collier, Jonathan A. Iggo, Robin Whyman *

Department of Chemistry, University of Liverpool, P.O. Box 147, Liverpool L69 7ZD, UK

Abstract

Solvent-stabilised Pt and Pd nanoparticles, of size range 2.3–2.8 nm and 2.7–3.8 nm, respectively, have been prepared by metal vapour synthesis routes, characterised by transmission electron microscopy (TEM), and their behaviour as catalysts for the enantioselective hydrogenation of ethyl pyruvate (EP) investigated; comparisons have been effected with the performance of standard supported Pt and Pd catalysts. Cinchona alkaloid-modified Pt nanoparticles display parallel behaviour to that exhibited by their conventional supported counterparts both in terms of the sense of the enantioselectivity in the ethyl lactate product and in the acceleration in reaction rate relative to the unmodified system. With Pd, however, significant differences are noted. Here, the sense of the enantioselectivity relative to that reported previously over conventional supported catalysts is reversed, i.e., an (R)- vs. (S)-enantiomer switch occurs, and a rate acceleration rather than retardation is noted on cinchona alkaloid modification. The Pt particle size distribution shows a higher degree of monodispersity after use in catalysis, although the average particle size remains essentially unchanged, whereas the behaviour of the Pd nanoparticles shows evidence of concentration dependence, lower concentrations showing Pt-like behaviour but more highly concentrated preparations showing evidence of significant aggregation during catalysis. With Pt catalysts, the presence of water as a component of the ketonic solvent system is shown to result in a significant acceleration in overall reaction rate with both conventional supported catalysts and their solvent-stabilised counterparts. In sharp contrast, totally aqueous-based colloidal platinum preparations, obtained by conventional salt reduction, display very low reaction rates and enantioselectivities. © 1999 Elsevier Science B.V. All rights reserved.

1. Introduction

The preparation and characterisation of metal nanoparticles is currently of considerable practical and theoretical interest because such materials fall into that intermediate state of matter between the molecular and the bulk and frequently display unusual physical (structural, electronic, magnetic and optical) and chemical (catalytic) properties [1,2]. As one aspect of our interests in this area, we have developed a reproducible method, using vapour synthesis techniques [3], for the production of solvent-

---

* Corresponding author. Fax: +44-151-794-3588; E-mail: whyman@liv.ac.uk

stabilised metal nanoparticles in the size range 2–3 nm. This has been applied to the preparation of Ru, Rh, Pd, Pt, Ag and Au nanoparticles; particle size characterisation has been effected by high resolution transmission electron microscopy (HRTEM). In terms of catalytic applications of such materials, we have previously reported the use of Au nanoparticles as precursors to supported gold catalysts for use in the low temperature oxidation of carbon monoxide [4]. Palladium and platinum are used extensively as selective heterogeneous hydrogenation catalysts; however, reports of their utilisation in the colloidal form for enantioselective hydrogenation are few [5–8]. In this work, we describe our recent results relating to the application of solvent-stabilised Pt and Pd nanoparticles, prepared by vapour synthesis routes, for the enantioselective hydrogenation of ethyl pyruvate, and a comparison of their behaviour with that of conventional oxide-supported catalysts.

The enantioselective hydrogenation of pyruvate esters catalysed by Pt modified by the cinchona alkaloids cinchonidine (CD) and cinchonine (CN), the Orito reaction, has received much attention recently as one of only a few effective heterogeneous enantioselective catalysts (Scheme 1) [9–12]. It is generally accepted that the adsorption of such modifiers onto a Pt surface via the quinoline moiety [13] provides an adjacent site at which selective enantioface adsorption of pyruvate occurs and at which subsequent hydrogenation provides lactate product with one enantiomer formed in excess, cinchonidine favouring the (R)-enantiomer and cinchonine the (S)-enantiomer. Concomitant with enantioselectivity is an increase in rate, the enantioselective reaction typically being 20 to 50 times faster than reaction in the absence of alkaloid. The corresponding Pd catalysed reactions have been less well studied [14–16]. Two distinctive features of the Pd-catalysed reaction are as follows: (i) the sense of the enantioselectivity is reversed with respect to that of the Pt system (i.e., CD directs the reaction to (S)-
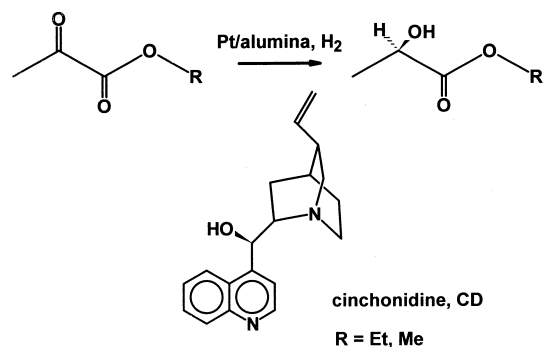
Scheme 1.

product and CN to the (R)-product), and (ii) there is not only no rate enhancement, but a slight retardation relative to that of the racemic reaction [14,15].

2. Results and discussion

2.1. Preparation and characterisation of solvent-stabilised Pt and Pd nanoparticles

Solvent-stabilised nanoparticles of Pt and Pd were prepared by the electron beam evaporation of the metals and co-condensation with the vapours of organic solvents at 77 K in a Torrovap metal atom reactor, as described previously [3]. Preferred solvents for the stabilisation of such nanoparticles are ketones, in particular, butan-2-one, methylethylketone (MEK), and acetone (MMK). The ready miscibility of acetone with water has been utilised to facilitate the preparation of nanoparticles in mixed organic/aqueous media and allows a ready comparison with the behaviour of more conventional aqueous-based colloidal systems. Additional proprietary stabilising agents KD1 and KD2 were also employed in some nanoparticle preparations. The solvent-stabilised Pt and Pd nanoparticles prepared and used in this catalytic investigation are summarised in Table 1, together with estimates of their particle sizes measured by TEM before and after evaluation of their catalytic behaviour.

Table 1

Particle size ranges measured from TEM analysis of a selection of solvent-stabilised nanoparticulate Pt and Pd pre- and post-catalyst testing in the enantioselective hydrogenation of ethyl pyruvate

Entry	Catalyst	Concentration (mmol dm^{-3})	Particle size range (nm $\pm \sigma$)	
			Pre-catalysis	Post-catalysis
1	Pt/MEK	1.3	2.3 ± 0.8	2.5 ± 0.7
2	Pt/MEK/KD1	17	2.5 ± 0.8	2.8 ± 1.03
3	Pt/MEK/KD2	3.8	2.5 ± 0.6	2.8 ± 0.7
4	Pt/MEK/CD	0.6	5.4 ± 1.3	2.2 ± 0.5
5	Pt/MMK/H$_2$O	4.6	2.6 ± 0.6	2.8 ± 0.6
6	Pt/MMK/H$_2$O/KD2	4.4	2.8 ± 0.9	2.4 ± 0.5
7	Pt/H$_2$O[a]	7.2	2.5 ± 0.6	3.4 ± 1.4
8	Pd/MEK/KD1	78	3.8 ± 1.1	5.4 ± 1.9
9	Pd/MEK/KD1[A]	28	3.0 ± 0.9	5.2 ± 1.9
10	Pd/MEK/KD1[B]	0.6	2.9 ± 0.9	3.5 ± 0.7
11	Pd/MEK/KD2	1.1	2.7 ± 0.8	17.4 ± 4.1

[a] Pt/H$_2$O prepared by reduction of aqueous chloroplatinic acid.

In general, the electron micrographs of the freshly prepared materials are of similar appearance and show a mixture of spatially well-separated primary particles with the size distributions indicated together with aggregates of these primary particles into larger 'clumps' having the appearance of 'frogspawn', 'raspberries' or 'caviar', depending on one's country of origin! This clumping phenomenon probably arises as a consequence of the convective forces that occur as the solvent evaporates from the specimen on the electron microscope grid, and is thus an artefact of the drying process rather than an intrinsic structural property of these materials. An alternative explanation is the presence of some metallo-organic component in addition to purely metallic states [3]. In some samples, e.g., Pt/MEK, Pt/MMK/H$_2$O, particularly those without the KD1 and KD2 stabilising agents, some evidence of agglomeration to bulk μm-sized material is frequently noted.

2.2. The enantioselective catalytic hydrogenation of ethyl pyruvate

2.2.1. Platinum catalysts

Solvent-stabilised Pt nanoparticles were tested for activity both before and after modification with either cinchonidine (CD) or cinchonine (CN) in the enantioselective hydrogenation (70 bar H$_2$, room temperature, 1 h) of ethyl pyruvate. Comparative experiments were also carried out using the standard heterogeneous silica-supported Pt catalyst, EUROPT-1. Representative results are summarised in Table 2 from which it can be concluded that these nanoparticulate catalysts, of sizes almost below the currently accepted size regime reported to exhibit enantioselectivity, display similar behavioural characteristics to their conventional supported counterparts. These include (i) rate enhancement in the presence of the modifier by factors in the range 50–85 for CD-modification, values which are significantly higher than observed previously in the majority of investigations using conventional heterogeneous catalysts, and (ii) the same direction of the enantioselectivity in the product ethyl lactate, i.e., (R)- and (S)-enantiomers following CD- and CN-modification, respectively (compare entries 1–3 with 4–6). It is also evident that they can display higher activity than conventional supported catalysts. The additional presence of the polymeric protecting agents KD1 and KD2 has only minor effects on reaction rate and ee for CN modification and a slight suppression of both with CD (entries 7–10). The lower level of enantioselectivity exhibited by the solvent-

Table 2
Initial rates of hydrogenation, EP conversions and ee's for CD- and CN-modified platinum catalysts used for the hydrogenation of ethyl pyruvate

Entry	Catalyst	Modifier	Initial rate $(\text{mmol s}^{-1} \text{ mol}_{\text{metal}}^{-1})$	Conversion (%)	ee (%)
1	EUROPT-1/MEK	CD	600	100	51(R)
2	EUROPT-1/MEK	CN	500	100	55(S)
3	EUROPT-1/MEK	–	25	32	0
4	Pt/MEK	CD	1025	100	25(R)
5	Pt/MEK	CN	830	100	15(S)
6	Pt/MEK	–	12	23	0
7	Pt/MEK/KD1	CD	634	100	12(R)
8	Pt/MEK/KD1	CN	795	100	12(S)
9	Pt/MEK/KD2	CD	496	100	14(R)
10	Pt/MEK/KD2	CN	655	100	13(S)
11	Pt/MEK/CD		133	31	14(R)

stabilised nanoparticles may reflect the relatively small particle sizes, ca. 2–3 nm, in these systems; previous reports have indicated that 3–4 nm is the minimum size requirement for good enantioselectivity [17]. Interestingly, however, in that report activity was also found to be optimal for particles larger than 3 nm. It is therefore possible that both the activity and enantioselectivity of the nanoparticulate materials prepared by the vapour synthesis route could be enhanced by increasing the particle sizes. Pre-modification by CD in the preparative stage is clearly deleterious to the observed reaction rate which approaches that of the unmodified catalysts (entry 11).

It is noteworthy that catalyst compositions which contain water as a significant component of the solvent mixture should show evidence of enhanced activity in comparison with other catalyst formulations examined (compare entries 1–6, Table 3 with entries 1–6, Table 2). A report by Augustine et al. [18] referred to the beneficial effects of traces of water on reaction rate but almost all the previous work in this area has used, nominally at least, organic solvents alone as reaction media. For the purposes of comparison, entries 7–9 in Table 3 illustrate the behaviour of nanoparticulate Pt catalysts prepared by conventional reduction of aqueous solutions of chloroplatinic acid. The resultant low

Table 3
Effect of water on catalytic activity and enantioselectivity during Pt-catalysed hydrogenation of ethyl pyruvate

Entry	Catalyst	Modifier	Initial rate $(\text{mmol s}^{-1} \text{ mol}_{\text{metal}}^{-1})$	Conversion (%)	ee (%)
1	Pt/MMK/H$_2$O[a]	CD	4198	100	26(R)
2	Pt/MMK/H$_2$O	CN	2253	100	36(S)
3	Pt/MMK/H$_2$O/KD2	CD	3110	100	22(R)
4	Pt/MMK/H$_2$O/KD2	–	57	21	0
5	EUROPT-1/MMK/H$_2$O	CD	1131	100	32(R)
6	EUROPT-1/MMK/H$_2$O	CN	456	100	19(S)
7	Pt/H$_2$O[b]	CD	67	79	13(R)
8	Pt/H$_2$O	CN	248	100	9(S)
9	Pt/H$_2$O	–	27	5	0

[a] MMK = acetone, MMK/H$_2$O = 4/1 v/v.
[b] Pt/H$_2$O catalyst prepared by reduction of aqueous chloroplatinic acid using hydroxylamine hydrochloride.

reaction rates, which approach those exhibited by the unmodified catalysts, may be accounted for, in part by the limited miscibility of ethyl pyruvate with water, notwithstanding the vigorous stirring rates used throughout the catalyst testing procedures. It should be noted that the particle size distribution pre-catalysis (Table 1, entry 7) is very similar to those of the other members of the Pt/MEK, Pt/MMK/H$_2$O series investigated.

In general, the morphologies of the solvent-stabilised Pt nanoparticles do not appear to be greatly affected by use in catalysis and little additional bulk agglomerated material is observed post-catalysis. Examination by TEM after catalyst testing reveals only a marginal increase in mean particle size from ca. 2.5 ± 0.7 to 2.7 ± 0.7 nm (see Table 1) although there is evidence of a greater extent of the 'clumping' phenomenon post-catalysis. This may be a consequence of the additional presence of traces of ethyl pyruvate and ethyl lactate (or their degradation products, possibly polymeric residues) which are less volatile than the solvents MEK, acetone, etc., used in the initial preparative stages. Nevertheless, the profile of the particle size distributions is in some cases 'sharpened' during the process of catalyst evaluation, for example, Pt/MEK (Fig. 1), and Pt/MEK/KD2, in the direction of a higher degree of monodispersity.

2.2.2. Palladium catalysts

In marked contrast to the catalytic behaviour displayed by Pt, solvent-stabilised Pd nanoparticles have been found to display some surprising, and at present unexplained differences, from conventional supported Pd catalysts towards the enantioselective hydrogenation of ethyl pyruvate (see Table 4). Thus CD-modified Pd nanoparticles also yield (R)-lactate with ee's of up to 30% in the hydrogenation of EP (entries 2, 3 and 6), i.e., in the *opposite* sense to that previously reported for CD-modified palladium catalysts. In further contrast to the behaviour of oxide-supported Pd catalysts, these reactions
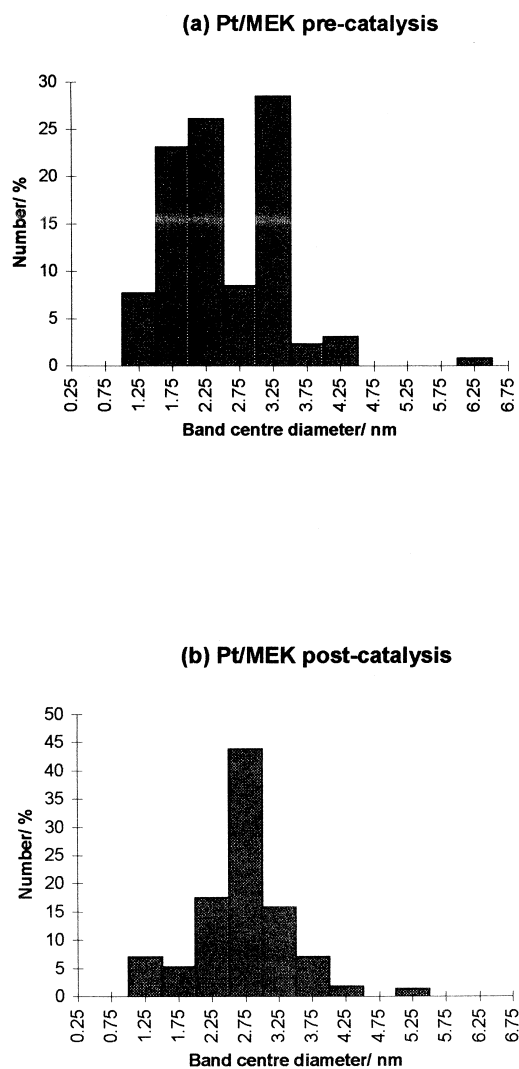

Fig. 1. Particle size distributions for Pt/MEK measured: (a) pre-catalysis, and (b) post-catalysis.

also appear to show rate enhancement, the rate of the unmodified reaction being very slow (compare entries 2–4 with 5). The enantioselectivity induced by CN is more muted, in agreement with previous reports that CN is a less effective modifier than CD, and is in favour of (S)-lactate (entries 4, 7). The behaviour of the solvent-stabilised Pd nanoparticles thus emulates platinum in terms of *both* the sense of the direction of enantioselectivity and in showing a rate enhancement in the enantioselective hydrogenation of pyruvate esters. It is noteworthy that

Table 4
Initial rates of hydrogenation, EP conversions and ee's for CD- and CN-modified palladium catalysts used for the hydrogenation of ethyl pyruvate

| Entry	Catalyst	Modifier	Initial rate (mmol s^{-1} mol$_{metal}^{-1}$)	Conversion (%)	ee (%)
1	Pd/C[a]	CD	n/r		14(S)
2	Pd/MEK/KD1[A]	CD	47	13	29(R)
3	Pd/MEK/KD1[B]	CD	130	13	7(R)
4	Pd/MEK/KD1	CN	17	8	12(S)
5	Pd/MEK/KD1	–	< 5	9	0
6	Pd/MEK/KD2	CD	101	18	9(R)
7	Pd/MEK/KD2	CN	17	8	3(S)
8	Pd/alumina[b]	CD	30	10	32(R)
9	Pd/alumina[b]	CN	17	6	7(S)

[a]Ref. [11].
[b]5% Pd/alumina Engelhardt ESCAT 14.

a standard Pd/alumina catalyst shows similar behaviour in MEK as solvent (entries 8, 9).

The solvent-stabilised Pd nanoparticles also provide a contrast with their Pt analogues in that the particle size distribution increases significantly in most cases during use in catalysis, typically increasing in the range from 2.9–3.8 nm pre-reaction to 3.5–5.4 nm post-reaction and increasing in dispersity (see Fig. 2, for Pd/MEK/KD1[A]). Nevertheless with Pd/MEK/KD1[B] (Fig. 3), the reverse situation, i.e., that which obtains for the majority of solvent-stabilised Pt nanoparticles, is observed, namely a redistribution and 'sharpening' of the particle size distribution. This difference may be a consequence of variation in Pd concentrations in the samples examined, the Pd concentration of Pd/MEK/KD1[B] at 0.6 mmol dm^{-3} being very much lower than that of Pd/MEK/KD1-[A], 28 mmol dm^{-3}. These differences in initial particle size distribution may also account for the differences in enantioselectivity noted in entries 2 and 3, the larger particles in catalyst [A] inducing higher levels of enantioselectivity, cf. Ref. [17]. In all cases examined, there is a higher degree of clumping, in some cases, occurring to such an extent that the primary particles appear to be spread across the specimen grid in the form of an interlinked network.

Further work is required in attempts to determine the origin of the observed switch in the sense of the enantioselectivity over palladium catalysts. The mechanistic pathway of palladium-catalysed reactions, in general, is much less well understood than the corresponding platinum-catalysed systems. Deuterium labelling experiments have shown that in contrast to Pt, over conventional oxide-supported Pd, the main product forming route is via the enol and carbon–carbon double bond hydrogenation [15].

(a) Pd/MEK/KD1 pre-catalysis
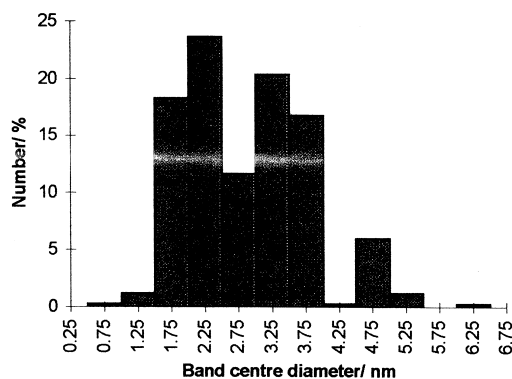
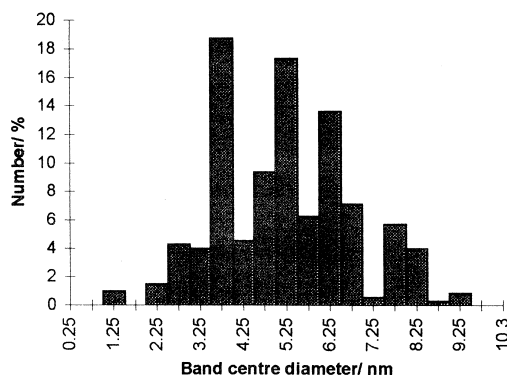

(b) Pd/MEK/KD1 post-catalysis

Fig. 2. Particle size distributions for Pd/MEK/KD1[A] measured: (a) pre-catalysis, and (b) post-catalysis.

(a) Pd/MEK/KD1 pre-catalysis

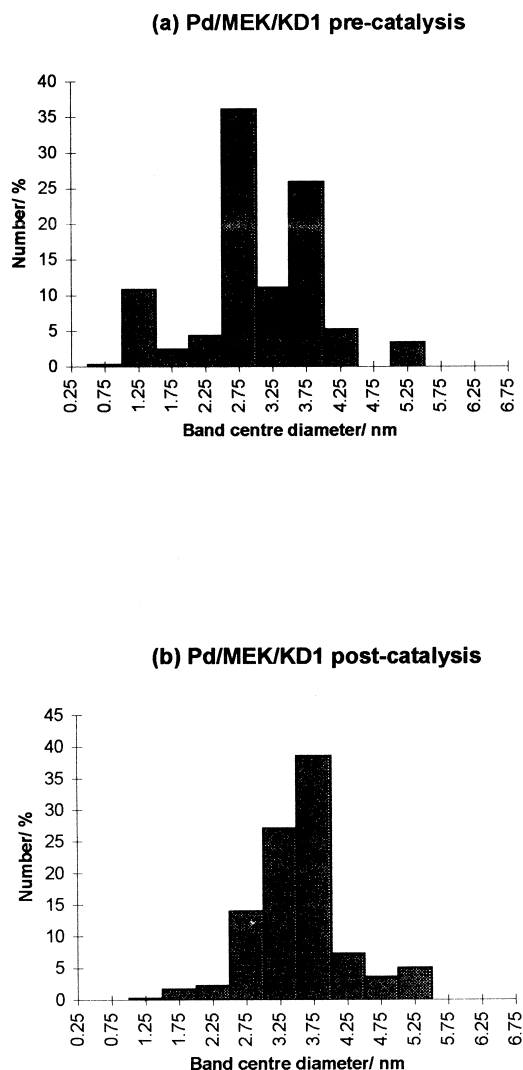### (b) Pd/MEK/KD1 post-catalysis

Fig. 3. Particle size distributions for Pd/MEK/KD1[B] measured: (a) pre-catalysis, and (b) post-catalysis.

It is however quite conceivable that carbon–oxygen double bond hydrogenation and carbon–carbon double bond hydrogenation via the enolate conformer may provide delicately balanced competitive mechanistic pathways with different Pd catalysts. Deuterium tracer experiments are in progress to test this possibility.

Recent collaborative work with the group of Prof. P.B. Wells has provided evidence that the situation with respect to catalysis by palladium is even more complex than indicated in the preliminary work reported here and that not only the *sense* of the enantioselectivity may be switched, but the outcome of the enantioselective hydrogenation of pyruvate esters may also be dependent on the choice of *both* solvent *and* substituent, e.g., R = Et or Me [19].

3. Conclusions

Some new and presently unexplained results have emerged from these preliminary studies with solvent-stabilised nanoparticles. The behaviour of solvent-stabilised Pt nanoparticles towards the enantioselective hydrogenation of ethyl pyruvate parallels that observed with conventional cinchona alkaloid-modified, oxide-supported Pt catalysts in respect of both (i) the acceleration in reaction rate relative to the unmodified system, and (ii) the sense of the enantioselectivity in the ethyl lactate product. In marked contrast, the use of solvent-stabilised Pd nanoparticles results in (i) a reversal of the sense of the enantioselectivity previously reported over conventional supported catalysts, and (ii) a rate acceleration rather than retardation on cinchona alkaloid modification. From this and other work, it has become evident that notwithstanding generally low activities and enantioselectivities, the Pd-catalysed enantioselective hydrogenation of ethyl pyruvate is much more complex than the corresponding Pt catalysed reactions. The substantial rate enhancement effect of the presence of water which has been observed with, for example, Pt/MMK/H_2O, appears new and is at present unexplained. In contrast, aqueous-based Pt nanoparticle preparations obtained by simple conventional chloroplatinic acid reduction show both low reaction rates and enantioselectivities. Although the metal particle size distributions remain relatively unchanged during catalysis with Pt, some variation in behaviour, which appears to be concentration dependent, is observed dur-

ing catalysis with solvent-stabilised Pd nanoparticles.

4. Experimental

4.1. Preparation of solvent-stabilised Pd and Pt nanoparticles

The solvent-stabilised nanoparticles listed in Table 1 were prepared by the evaporation of platinum and palladium metals and co-condensation of their vapours with those of organic solvents at 77 K using a commercial positive hearth electrostatically focused electron beam rotary metal atom reactor (Torrovap Industries, Ontario, Canada) as described previously [3].

Typically, 2.5 g of KD1, a proprietary polymeric protecting agent in the Hypermer KD range of dispersants marketed under the Solsperse tradename by Zeneca Colours, was melted and dispersed onto the walls of the 5 l spherical reactor chamber, after which it was evacuated to 10^{-7} Torr and cooled in liquid nitrogen. Palladium (11.3 mmol) was then evaporated over 2 h and co-condensed with butan-2-one (MEK) (145 cm^3) which was simultaneously added to the vessel as vapour. After deposition the chamber was slowly warmed to room temperature during which period a further 2.5 g of KD1 in 60 cm^3 of MEK was added to the softening matrix of reactants. After warming to room temperature, the resultant clear brown liquid was transferred under anaerobic conditions into a Schlenk receiver vessel for storage.

Solvent-stabilised nanoparticles of Pt were prepared by a similar procedure. One Pt sample was prepared in the presence of the alkaloid cinchonidine as a stabilising agent (Table 1, entry 4). This was achieved by first coating the walls of the rotating reaction chamber with a dichloromethane solution of cinchonidine followed by evaporation of the solvent under vacuum. The product was then obtained after co-condensation of platinum and MEK vapours onto the cinchonidine layer at 77 K, followed

by slow warming to room temperature and workup using the procedure described above.

4.2. Characterisation of solvent-stabilised metal nanoparticles

Metal concentrations of the solvent-stabilised nanoparticles were determined by atomic absorption spectroscopy (AAS).

Particle sizes and morphologies of the solvent-stabilised nanoparticles, both in the as-prepared state and after use as catalysts for enantioselective hydrogenation, were determined by transmission electron microscopy (TEM). Phase contrast TEM images were obtained using a side entry Philips EM400 electron microscope operating at 120 kV. Specimens were prepared by allowing one or two drops of the sample solution to evaporate onto a standard copper grid (supplied by Agar Scientific).

For particle size analysis and construction of the histograms of particle size distributions, at least 300 particles were measured from each micrograph obtained from different areas of the sample grid and at various magnifications.

4.3. Catalytic hydrogenation studies

Solutions of the solvent-stabilised palladium nanoparticles containing either 1.8 mg Pt or 1 mg of Pd, CD or CN modifier (6 mg, 2×10^{-5} mol), freshly distilled ethyl pyruvate (Aldrich) and solvent (total reaction volume: 20 cm^3) were added to a Parr Model No. 4592 autoclave. The autoclave was sealed, purged three times with H$_2$ to 50 bar and then pressurised to 70 bar with H$_2$ and maintained at 25 ± 1°C for 1 h. Rates of reaction were determined from hydrogen uptake data measured during the period of steady reaction using a pressure transducer fitted to the autoclave.

At the conclusion of the reactions, the product solutions were analysed for substrate conversion and ee by GC, using an FFAP capillary column (Alltech) and a CDX-B capillary chiral column (J&W Scientific), respectively. For ee

determination, the product solution was analysed following derivatisation with trifluoroacetic anhydride.

Acknowledgements

References

[1] See, for example, G. Schmid (Ed.), Clusters and Colloids, VCH, Weinheim, 1994.
[2] W.A. deHeer, Rev. Mod. Phys. 65 (1993) 611.
[3] R.W. Devenish, T. Goulding, B.T. Heaton, R. Whyman, J. Chem. Soc., Dalton Trans. (1996) 673.
[4] G.J. Hutchings, M.R.H. Siddiqui, A. Burrows, C.J. Kiely, R. Whyman, J. Chem. Soc., Faraday Trans. 93 (1997) 187.
[5] P.J. Collier, T. Goulding, J.A. Iggo, R. Whyman, in: G. Jannes, V. Dubois (Eds.), Chiral Reactions in Heterogeneous Catalysis, Plenum, NY, 1995, p. 105.
[6] J.U. Kohler, J.S. Bradley, Catal. Lett. 45 (1997) 203.
[7] J.U. Kohler, J.S. Bradley, Langmuir 14 (1998) 2730.
[8] X. Zuo, H. Liu, M. Liu, Tetrahedron Lett. 39 (1998) 1941.
[9] P.B. Wells, A.G. Wilkinson, Top. Catal. 5 (1998) 39.
[10] A. Baiker, J. Mol. Catal. A 115 (1997) 473.
[11] H.-U. Blaser, H.P. Jalett, M. Muller, M. Studer, Catal. Today 37 (1997) 44.
[12] R.L. Augustine, S.K. Tanielyan, J. Mol. Catal. A 118 (1997) 79.
[13] G. Bond, P.B. Wells, J. Catal. 150 (1994) 329.
[14] H.-U. Blaser, H.P. Jalett, D.M. Monti, J.F. Reber, J.T. Wehrli, Stud. Surf. Sci. Catal. 41 (1988) 153.
[15] T.J. Hall, P. Johnston, W.A.H. Vermeer, S.R. Watson, P.B. Wells, Stud. Surf. Sci. Catal. 101 (1996) 221.
[16] T. Mallat, S. Szabo, M. Schurch, U.W. Gobel, A. Baiker, Catal. Lett. 47 (1997) 221.
[17] J.T. Wehrli, A. Baiker, D.M. Monti, H.-U. Blaser, J. Mol. Catal. 61 (1990) 207.
[18] R.L. Augustine, S.K. Tanielyan, L.K. Doyle, Tetrahedron: Asymmetry 4 (1993) 1803.
[19] P.J. Collier, T.J. Hall, J.A. Iggo, P. Johnston, J.A. Slipszenko, P.B. Wells, R. Whyman, J. Chem. Soc., Chem. Commun. (1998) 1451.